VILNIUS TECH
Vilnius Gediminas Technical University

Proceedings of the 13th International Scientific Conference

ENVIRONMENTAL ENGINEERING

April 23–24, 2026, Vilnius, LITHUANIA

eISSN 2029-7092
eISBN 978-609-476-444-8
Article ID: enviro.2026.1448
https://doi.org/10.3846/enviro.2026.1448

EFFECT OF PERFORATION HOLE SHAPE AND ANGLE ON SOUND ABSORPTION IN PERFORATED PLASTIC PANELS

Tomas ASTRAUSKAS*, Robert RUŽICKIJ, Andrej NAIMUŠIN, Jolita BRADULIENĖ, Mantas PRANSKEVIČIUS, Tomas JANUŠEVIČIUS

Vilnius Gediminas Technical University, *Vilnius*, *Lithuania*

Received 23 January 2026; revised 18 February 2026; accepted 24 February 2026

Abstract. This study investigates the influence of hole shape on the sound absorption performance of perforated plastic panels. Circular, square, diamond, and teardrop curve shapes were selected for this study. A series of experimental measurements were conducted using the standard impedance tube transfer function method. The acoustic behaviour of each configuration was analysed in the 50–5000 Hz frequency range. The results indicate that the shape of the perforation holes significantly affects the absorption characteristics, particularly in the high-frequency range. Panels with optimised geometries demonstrated enhanced sound absorption, suggesting that the shape of the perforation hole can improve the acoustic efficiency of lightweight plastic materials. The thickness of all panels and the hole size were kept constant to 20,0 and 3,0 mm, respectively. For all perforation hole shapes, results showed that the sound absorption peak was achieved at 4000 Hz. The highest peak sound absorption was 0.85 when measured on a panel with holes of the shape of square. The aim of this study was to find the correlation between sound absorption and the shape of the perforation hole.

Keywords: sound absorption, perforated panels, perforation hole shape, impedance tube.

1. Introduction

Noise pollution is a complex public health, environmental quality, and economic productivity problem. Its control demands multiple solutions involving scientists, government, and innovations (Aliyev et al., 2025; Del Pozo et al., 2024; Eren et al., 2024; Swinburn et al., 2015). Sound absorbing materials – ranging from traditional fibrous and porous types composites (S. Dong et al., 2024; Mohammadi et al., 2025), acoustic metamaterials (Groby et al., 2021; Naimušin & Januševičius, 2023) and perforated (Khosravani & Reinicke, 2021; Xie & Lyu, 2014) or micro perforated (Herrin et al., 2011; Tang & Cheng, 2025) panels often used for mitigation of noise pollution. The integration of environmentally friendly materials with advanced design and manufacturing techniques could align noise control with broader sustainability goals.

Sustainable materials for sound absorption applications often include natural fibres such as jute, coconut coir, bamboo, sheep wool, and biobased composites with Polylactic acid (PLA) or epoxy with natural fibres (Khosravani & Reinicke, 2021; Mohammadi et al., 2025; Tang & Cheng, 2025). These materials often show attractive non-acoustic parameters such as thickness, density, porosity, which can be optimised through material composition optimisation. Emerging technologies such as machine learning-based design are improving durability, moisture resistance, and broadband acoustic performance, especially at low frequencies, while reducing environmental impact compared to conventional synthetic absorbers.

Resonant acoustic sound absorbers include Helmholtz resonators, micro-perforated panels, membrane-based absorbers, and advanced acoustic metamaterials. Hybrid and multi-layer designs achieve broadband low-frequency absorption in compact, subwavelength thicknesses by exploiting coupled resonances and advanced optimisation strategies. Peak sound absorption coefficients often exceed 0.9 in tuned frequency range, with bandwidths ranging from 100 Hz to several kHz, and thicknesses as low as 1/50 of the wavelength (Cai & Xin, 2025; Zhao et al., 2025).

The sound absorption of perforated panels (PP) depends on the geometric optimisation of the material. The shape of the perforation holes is one of the most important factors in optimising sound absorption for different frequency ranges. Designs that are in market often favour circular holes because of the simplicity of

* Corresponding author. E-mail: *tomas.astrauskas@vilniustech.lt*

the manufacturing. The other shapes of holes have different acoustic benefits (Su et al., 2021). For example, square and triangular hole shapes increase airflow resistivity compared to circle-shaped holes. The increase in sound absorption effectiveness is approximately 11–12% (Dorra et al., 2021). Elliptical-shaped holes make perforated panels more universal for applications. The incident angle does not affect sound absorption of the perforated panel (Bocanegra et al., 2024). Slotted holes extend the bandwidth of sound absorption, especially when thin panels are used with a high perforation ratio (Jiang et al., 2024). Panels with tapered holes and porous backing increase sound absorption in low mid frequencies (Patil et al., 2024).

Few studies have shown that increasing the angle of the perforation hole can enhance sound absorption. For example, a study on perforated plastic or wood panels with tilted holes (15° to 45°) showed that the sound absorption coefficient (SAC) and transmission loss (TL) increased with the angle of the perforation pore (Astrauskas et al., 2024). Furthermore, studies show that tilt angle allows to shift resonant frequency of the sound absorption (Dong et al., 2020). This suggests that tilting the perforations can improve the acoustic performance of the PP.

This paper aims to investigate the influence of different hole shapes on SAC. In this paper, we investigate circular, square, diamond, and teardrop curve shapes. This study essentially incorporates all the studies mentioned into one. Different shapes of perforation holes are combined with the tilt angle to achieve the optimal performance of the existing perforation; therefore, some different shapes were analysed in this study. Compared to other studies, the perforation hole tilt angle was increased to 60° to potentially improve sound absorption.

The paper is organised as follows: in section 2 Materials and methods presented; in section 3 The main results; In section 4 discussion of the result; In section 5 the results were concluded.

2. Materials and methods

To produce perforated panels the 3D printing technology was used, because such panels need precision to be produced for laboratory scale testing. To ensure equal conditions, some parameters of the panels were kept constant: thickness (20 mm), hole diameter (3 mm), the distance between holes (9 mm – centre to centre of the hole). The perforation matrix is constant in all dimensions. The controlled parameters in this study were the shape of the hole and the tilt angle. The shapes selected for this study were circular (Figure 1a), square (Figure 1b), diamond (Figure 1c), and teardrop curve (Figure 1d) shapes.

The tilt angles in comparison to sound incidence angle were 15°; 30°; 45°; 60°. The tilting angle allows to increase the tortuosity values of perforated hole; therefore, it leads to higher sound absorption values.

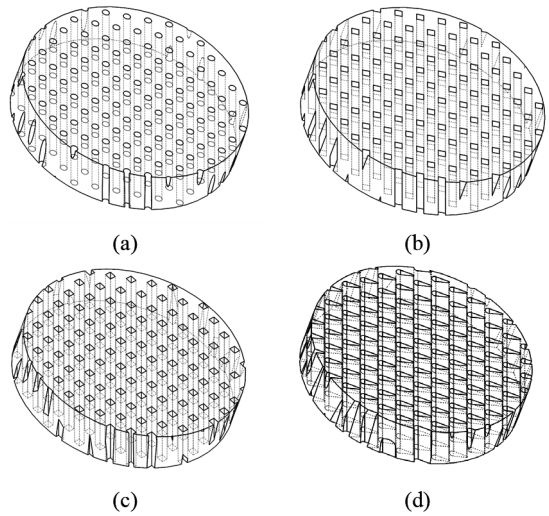

Figure 1. Drawing of the panels with different perforated hole shapes: (a) – circle; (b) – square; (c) – diamond; (d) – teardrop

To obtain the sound absorption coefficient (α) of PP, the ISO 10534-2 standard method was used. Such a method was chosen due to the requirements for sample size compared with methods which can be performed in reverberant rooms. The two impedance tubes used in the study were manufactured by Gesellschaft für Akustikforschung Dresden GmbH, AcoustiTube product. The three-microphone technique was implemented to obtain less noisy data. Two tubes allowed to measure SAC in the wider frequency range. For lower frequency range (50–2000 Hz) measurements, a 100 mm inner diameter tube was used, while for higher frequency range (150–5000 Hz) a 30 mm inner diameter tube. The experimental setup with a 30 mm inner diameter tube is shown in Figure 2. The total measured frequency range was 50–5000 Hz. The white noise signal was used in this study because it contains equal energy across the frequency range, allowing simultaneous measurement of the acoustic properties of materials without performing multiple single-frequency tests. This approach significantly reduces measurement time while maintaining accuracy.

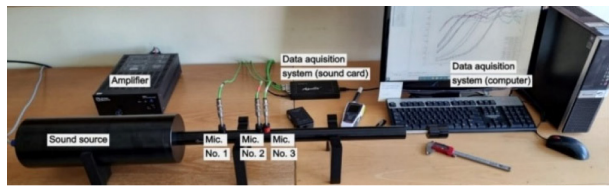

Figure 2. The impedance tube configuration for sound absorption measurements

The transfer function H_{13} between microphone positions is calculated as the pressure ratio between pressures measured by both microphones (Eq. (1)). The transfer function for incident wave H_I and transfer function for

reflected wave H_R calculated according to (Eq. (2)–(5)) (International Organization for Standardization, 2001)

$$H_{13} = \frac{p_3}{p_1}, \quad H_{23} = \frac{p_3}{p_2}; \tag{1}$$

$$H_{I(mic1-3)} = \frac{p_{3I}}{p_{1I}} = e^{-jk_0(x_{12}+x_{23})}; \tag{2}$$

$$H_{I(mic2-3)} = \frac{p_{3I}}{p2_I} = e^{-jk_0(x_{23})}; \tag{3}$$

$$H_{R(mic1-3)} = \frac{p_{3R}}{p_{1R}} = e^{jk_0(x_{12}+x_{23})}; \tag{4}$$

$$H_{R(mic2-3)} = \frac{p_{3R}}{p_{1R}} = e^{jk_0(x_{23})}. \tag{5}$$

From Eq. (6), (7) the reflection coefficient of the sample can be calculated as:

$$R_{(mic1-3)} = \frac{H_{13} - H_{I(mic1-3)}}{H_{R(mic1-3)} - H_{12}} e^{2jk_0(X_{12}+X_{23}+X_{3s})}; \tag{6}$$

$$R_{(mic2-3)} = \frac{H_{23} - H_{I(mic2-3)}}{H_{R(mic2-3)} - H_{13}} e^{2jk_0(X_{23}+X_{3s})}, \tag{7}$$

where: R is the reflection coefficient of the sample, k_0 is the wave number in air.

Finally, the sound absorption coefficient (α) is calculated using the following expression:

$$\alpha = 1 - |R|^2. \tag{8}$$

For engineering applications, sound spectra are often presented as one-third octave frequency bands rather than narrow bands. This frequency representation is related to the perception of sound by the human ear and allows compression of the amount of information. In this paper, the results are presented in 1/3 octave to show relevant information while focussing on the application possibilities of the panels.

To summarise results the decision was made to introduce averaged sound absorption coefficient which is calculated according to a Eq. (8):

$$\alpha_{avg} = \frac{\sum \alpha_n}{n}, \tag{9}$$

where: α_{avg} – averaged sound absorption coefficient; α_n – sound absorption coefficient in n^{th} 1/3 octave band; n – number of octave bands (50–5000 Hz; n = 21).

The PP was 3D printed and the print accuracy is 0.01 mm. Knowing that to save resources, only one sample was printed for each configuration. The possible variations in terms of sound absorption are negligible. Therefore, operator uncertainty is only a variable that influences the measurement accuracy. The uncertainty of the operator was calculated as standard deviation of 15 independent measurements of the same operator and is presented in Table 1.

Table 1. The operator uncertainty of the measurement

Frequency, Hz	Uncertainty, σ
50	0.005
63	0.002
80	0.001
100	0.004
125	0.006
160	0.007
200	0.005
250	0.004
315	0.002
400	0.002
500	0.004
630	0.006
800	0.009
1000	0.009
1250	0.009
1600	0.023
2000	0.014
2500	0.010
3150	0.010
4000	0.007
5000	0.014

To ensure accurate SAC data, 100 averages were made for each measurement. In total, 8 separate samples were tested to obtain the SAC data.

3. Results

In this section results of sound absorption of perforated panels are presented.

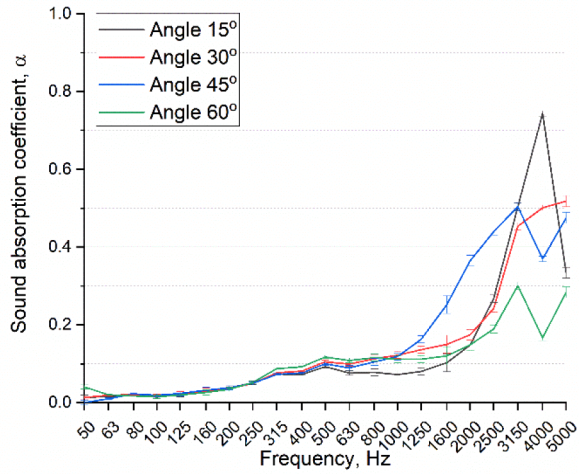

Figure 3. Frequency dependent sound absorption coefficient of circular perforated panel

Figure 3 shows the frequency-dependent sound absorption coefficient (α) of a circular shape perforated panel of different perforation hole tilting angles: 15°, 30°, 45° and 60°.

In all designs, this value of the sound absorption coefficient is low (α < 0.05) for low frequencies below 500 Hz, which means that low frequency absorption is relatively weak regardless of the angle of the perforation hole. In frequencies higher than 1000 Hz, sound absorption starts to vary between configurations.

Between 1000 and 2500 Hz the absorption curves increase similarly for all angles, but at 45° the value of α increases more distinct manner compared to other configurations. In frequency range 2500–3000 Hz sound absorption values were higher than 0.4, being higher compared with other angle configurations.

At 3000 to 5000 Hz, there is a considerable deviation of the values of the sound absorption coefficients. Resonant absorption is observed at this frequency, with a sharp peak reaching α ≈ 0.73 for the 15° tilt. The smoother transition is seen with a tilt of 30° for which α ≈ 0.52 is achieved. The 45° angle keeps moderate sound absorption, but at lower frequency 2500 Hz. The opposite is true in the case of a 60° tilt, which has a lower efficiency in terms of high frequency with its α ≈ 0.35 in the upper frequency range.

The results show that circular perforation hole tilt angle has a significant effect on the acoustic behaviour of the panel. Moderate tilting (30–45°) increases mid-frequency absorption, and shallow tilt angles (15°) can lead to high-frequency peak.

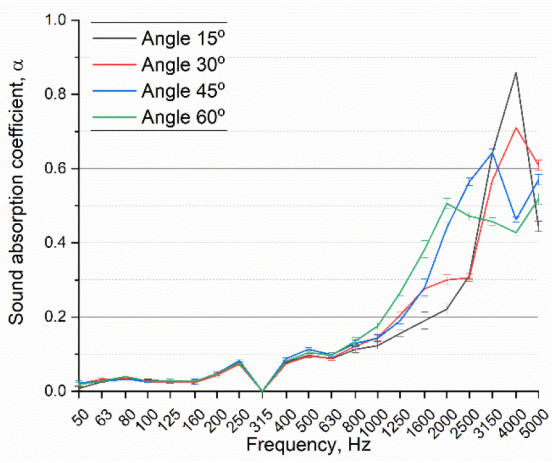

Figure 4. Frequency dependent sound absorption coefficient of square perforated panel

In Figure 4 presented the frequency-dependent sound absorption coefficient (α) of a perforated panel of different perforation hole tilting angles: 15°, 30°, 45° and 60°. The difference in sound absorption of panels with different perforation hole tilting angles is negligible in frequency range below 630 Hz.

A more distinct difference in sound absorption values is found in the 1 kHz to 2 kHz range. The highest values in this frequency range were found when measured panels with 60° tilt angle, reaching α ≈ 0.5 at around 2000 Hz, outperforming the other tilt angles. The 45° angle sound absorption increases similarly, though with a slightly lower value. Meanwhile, the 15° and 30° configurations show slower growth in absorption in this region.

In frequencies higher than 2000 Hz, the tilting angle effect is more noticeable. The 15° tilt angle panel exhibits a sharp rise, reaching its maximum absorption (0.83) at 4000 Hz, representing the strongest peak across all configurations. The 30° angle also shows a pronounced peak around the same frequency, but with a slightly lower amplitude (α ≈ 0.65). The 45° and 60° angles reach their peaks in a lower frequency range and values compared to the 30° and 15° cases.

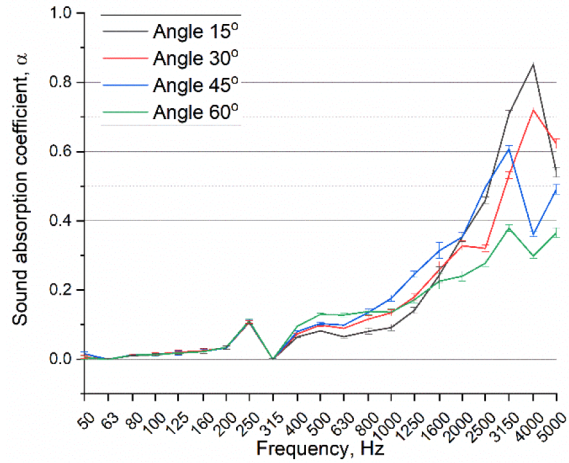

Figure 5. Frequency dependent sound absorption coefficient of diamond shaped holes perforated panel

Figure 5 presents the measured sound absorption coefficient (α) of a diamond-shaped perforated panel for four perforation hole tilt angles. At low frequency range (below 800 Hz), similarly to other configurations, low absorption without any significant differences.

Between 500 and 2000 Hz, the absorption coefficient begins to increase gradually for all tilt angles. Within this range, steeper tilting (45° and 60°) produces slightly higher absorption levels compared to the shallower 15° and 30° orientations. Such results show that sound absorption in medium to high frequency range is better achieved with steeper perforation hole angles.

More pronounced differences among the tested configurations occur above 2000 Hz. The 30° tilt angle exhibits a strong increase in absorption, reaching approximately α ≈ 0.65 at 4000 Hz. An even larger high-frequency peak was found for the 15° tilt angle, which peaks at about α ≈ 0.84 at 4000 Hz. This represents the highest absorption level among all investigated angles. The 45° and 60° orientations show more moderate peak values, on the order of α ≈ 0.35 – 0.60, indicating reduced high-frequency coupling compared to the shallower orientations.

This behaviour suggests that shallower tilting enhances the formation of high-frequency resonances associated with the effective cavity–neck system created by diamond – shaped openings.

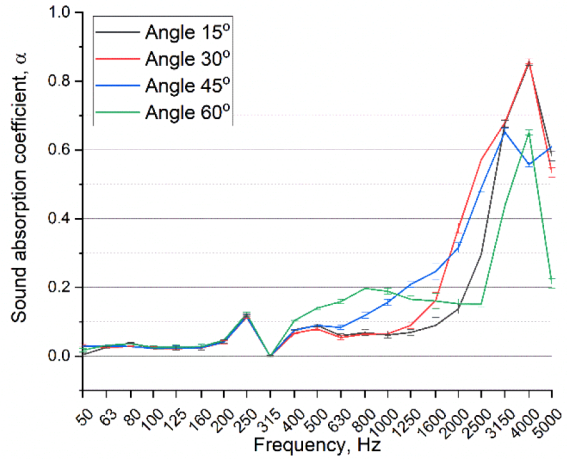

Figure 6. Frequency dependent sound absorption coefficient of teardrop curve shaped holes perforated panel

Figure 6 presents the measured sound absorption coefficient (α) of a perforated panel shaped by a teardrop curve. At low frequencies, all configurations showed low sound absorption values.

As the frequency increases toward the mid-frequency region (400–2000 Hz), the absorption coefficients begin to differ more noticeably between tilt angles. The 60° tilt angle results show the highest absorption in this frequency range, reaching α ≈ 0.20 at frequency of 800 Hz. The 15° and 30° angles maintain comparatively lower absorption values in this frequency range.

The most prominent differences between tilt angles appear in the high-frequency region (2000–5000 Hz). The 15° and 30° tilt angles demonstrate the best overall performance, showing a pronounced peak of approximately α ≈ 0.83 at 4000 Hz. The 45° angle reaches a moderate maximum of about α ≈ 0.66 at 3150 Hz, while the 60° orientation, despite its superior mid-frequency performance, displays a relatively reduced peak α ≈ 0.65 at 400 Hz. These results indicate that shallow tilt angles (15°–30°) promote stronger resonance formation in teardrop curve-shaped hole, whereas steep angles tend to suppress high-frequency resonance due to increased flow resistance and reduced effective coupling with the acoustic field.

To summarise the results, the heatmap graph is presented in Figure 7. Across all geometries, the results indicate that both shape and tilt angle significantly influence α_{avg}. Circular holes consistently yield the lowest values (0.104–0.158), with a 60° pronounced decrease at a tilt angle. Diamond-shaped holes showed comparatively higher values at lower tilt angles, reaching a maximum of 0.186 at 15°, and decreased to 0.133 at 60°. The teardrop-shaped hole-perforated panel showed relatively stable values (0.145–0.186) and a slight increase at 60°. Square holes showed the highest values (0.171–0.191), reaching their peak at 45°.

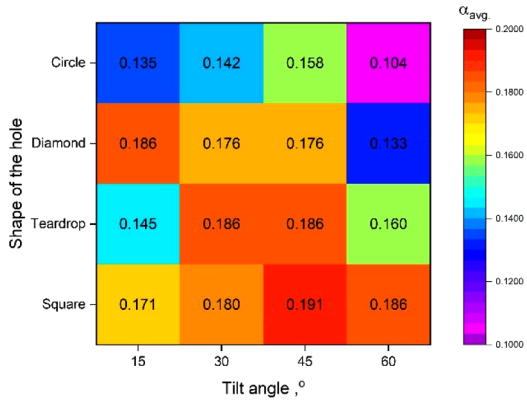

Figure 7. Heatmap graph of sound absorption coefficient average

A common trend is observed in most geometries: 45° tilt angles generally correspond to the highest α_{avg} values. At 60°, however, all shaped holes showed a reduced average sound absorption coefficient, indicating that excessively high tilt angles may not allow the sound wave to enter a sample but rather be reflected.

Overall, the averaged results demonstrate a clear interaction between geometric features and angular orientation. Square and diamond shapes tend to promote higher α_{avg} values, particularly at moderate tilt angles, while circular geometries consistently produce the lowest averaged sound absorption coefficients.

4. Discussion

For applications targeting upper mid to high frequencies (≈1–4 kHz) – e.g., speech clarity – teardrop curve and square shapes could be preferred. To extend absorption toward lower frequencies, the geometric shape alone is insufficient; adding a backing air cavity, increasing thickness, or re-tuning the perforation parameters (open area, spacing) would be required.

According to previous studies, the angle of the perforation hole increases the tortuosity of perforated panel. Compared to other studies the results do not correlate the same way as in other studies. The main reason is that other studies used a smaller diameter perforation hole; therefore, it was closer to microperforated panel; thus, higher acoustic pressure is within the perforated hole.

The different shapes of the perforation holes contribute to differences in acoustic impedances, as well as sound absorption itself (Ning et al., 2016). Such results were also shown in this study. Due to changes in the shape of the perforation hole it was possible to get slightly different sound absorption results.

The main limitation of this study was that not all full perforated holes fit within the sample area. Some holes

are cut in half due to the circular cross section of the sample, as shown in Figure 1. This limitation could lead to slightly lower values of sound absorption coefficient, because of the reduced open area than projected. In the future this limitation will be addressed using an infinite size sample using empirical model (Delany – Bazley). This limitation will also be eliminated when bigger scale samples will be produced in future research.

To enhance the sound absorption, porous backing or airgap could be introduced behind the PP. Future studies will include environmentally friendly sound-absorbing material backing and airgap optimisation.

5. Conclusions

The overall tendency shows that the tilting angle allows one to control frequency range for more efficient sound absorption. The results show that higher tilt angles (45° and 60°) allowed higher sound absorption in the frequency range from 500–2000 Hz. The lower tilt angle showed higher peak absorption in the higher frequency range.

Teardrop curve and square shape perforated panels showed the highest peak absorption $\alpha \approx 0.83$ and 0.84 respectively in frequency range above 2000 Hz. Diamond shape perforated panels showed stable, smooth growth with peak sound absorption reaching up to 0.84 but did not increase mid-frequency sound absorption with higher tilt angles. The circle shape perforation hole panels showed lowest peak sound absorption of all configurations. The peak sound absorption was somewhat effective only with 15° tilting angle and reached 0.73, other configurations of circular shape perforated panels showed maximum peak of 0.50.

The geometry and tilt angle of the perforated panel strongly influence the averaged sound absorption coefficient α_{avg}. The square and teardrop-shaped perforated panel generally showed the highest values, reaching 0.191 and 0.186 respectively at the 45° tilt angle. Circular holes consistently yield the lowest values at all angles (0.104–0.135). The perforated panels without taking into account the hole shape showed a peak of α_{avg} at 45 ° and a reduction at 60°, indicating that high tilt angles may not allow the sound wave to enter a sample but rather be reflected.

Funding

Research was conducted as part of the execution of Project “Mission-driven Implementation of Science and Innovation Programmes” (No. 02-002-P-0001), funded by the Economic Revitalization and Resilience Enhancement Plan “New Generation Lithuania”.

References

Aliyev, A. A., Nurubeyli, T. K., Haziyev, Y. H., Valiyev, S. M., Najafov, E. T., & Mammadov, F. I. (2025). Innovative noise mitigation techniques in transportation systems: Toward sustainable urban mobility. *International Journal on Technical and Physical Problems of Engineering*, *17*(2), 142–151.

Astrauskas, T., Grubliauskas, R., & Januševičius, T. (2024). Optimization of sound-absorbing and insulating structures with 3D printed recycled plastic and tyre rubber using the TOPSIS approach. *Journal of Vibration and Control*, *30*(7–8), 1772–1782. https://doi.org/10.1177/10775463231171218

Bocanegra, J. A., Borelli, D., Pallavidino, E., Peshku, J., & Schenone, C. (2024). Effects of geometric parameters on sound absorption in perforated plates with elliptical holes. In *Proceedings of the Annual Congress of International Institute of Acoustics and Vibration* (*IIAV*) (pp. 1–7). IRIS UniGe.

Cai, C., & Xin, F. (2025). Pressure-adaptive ultra-thin hybrid metamaterials for broadband low-frequency underwater sound absorption. *Thin-Walled Structures*, *216*, Article 113603. https://doi.org/10.1016/j.tws.2025.113603

Del Pozo, D. E., Donoso, N. C., & Valle, B. G. (2024). Mapping and mitigating urban noise: A case study of Loja, Ecuador’s soundscape. *Canadian Acoustics – Acoustique Canadienne*.

Dong, M., Jia, S., Liu, J., Lin, X., Xue, Q., & Sun, W. (2020). 穿孔⊠斜角度⊠3D打印仿生木材吸声⊠构的吸声性能影响 [Properties of 3D printed bionic wood sound absorption structure with different hole angles]. *Linye Kexue Scientia Silvae Sinicae*, *56*(5), 113–117. https://doi.org/10.11707/j.1001-7488.20200513

Dong, S., Duan, Y., Chen, X., You, F., Jiang, X., Wang, D., Hu, D., & Zhao, P. (2024). Recent advances in preparation and structure of polyurethane porous materials for sound absorbing application. *Macromolecular Rapid Communications*, *45*(14). https://doi.org/10.1002/marc.202400108

Dorra, H. M. A., Abd-Elbasseer, M., Mahmoud, A. E. A., & Mohamed, H. Kh. (2021). Influence of different distribution patterns of holes on single micro-perforated panel sound absorption behaviour. *Canadian Acoustics – Acoustique Canadienne*, *49*(2), 11–20.

Eren, B., Likos, S., & Çelebi, A. (2024). Effectiveness of noise barriers in sensitive urban areas: A comprehensive study on noise reduction strategies and public health implications. *Environmental Science and Pollution Research*, *31*(50), 60093–60107. https://doi.org/10.1007/s11356-024-35229-y

Groby, J. P., Jiménez, N., & Romero-García, V. (2021). Acoustic metamaterial absorbers. In N. Jiménez, O. Umnova, & J. P. Groby, *Acoustic waves in periodic structures, metamaterials, and porous media*. *Topics in Applied Physics* (Vol. 143, pp. 167–204). Springer Science and Business Media Deutschland GmbH. https://doi.org/10.1007/978-3-030-84300-7_5

Herrin, D., Liu, J., & Seybert, A. (2011). Properties and applications of microperforated panels. *Sound and Vibration*, *45*(7), 6–9.

International Organization for Standardization. (2001). *Acoustics – determination of sound absorption coefficient and impedance in impedance tubes* (ISO 10534-2). ISO.

Jiang, C., Li, X., Hu, W., & Wang, F. (2024). Micro-perforated plates constructions with approaching the theoretical limits of its sound absorption performance. *INTER-NOISE and*

NOISE-CON Congress and Conference Proceedings, *270*(7), 4389–4400. https://doi.org/10.3397/IN_2024_3453

Khosravani, M. R., & Reinicke, T. (2021). Experimental characterization of 3D-printed sound absorber. *European Journal of Mechanics – A/Solids*, *89*, Article 104304. https://doi.org/10.1016/j.euromechsol.2021.104304

Mohammadi, M., Ishak, M. R., Hameed Sultan, M. T., & Zainudin, E. S. (2025). Cutting-edge innovations in sound absorption properties of natural fiber reinforced polylactic acid composites. *Journal of Reinforced Plastics and Composites*. https://doi.org/10.1177/07316844251352718

Naimušin, A., & Januševičius, T. (2023). Development and research of recyclable composite metamaterial structures made of plastic and rubber waste to reduce indoor noise and reverberation. *Sustainability*, *15*(2), Article 1731. https://doi.org/10.3390/su15021731

Ning, J. F., Ren, S. W., & Zhao, G. P. (2016). Acoustic properties of micro-perforated panel absorber having arbitrary cross-sectional perforations. *Applied Acoustics*, *111*(2), 135–142. https://doi.org/10.1016/j.apacoust.2016.04.012

Patil, C., Ghorpade, R., & Askhedkar, R. (2024). Analysing the impact of 3D-printed perforated panels and polyurethane foam on sound absorption coefficients. *Modelling*, *5*(3), 969–989. https://doi.org/10.3390/modelling5030051

Su, Y., Lyu, Y., Yang, J., & Cheng, X. (2021). Design and experimental study of a highly efficient sound absorbing composite structure based on the perforated panel resonator with flexible tube bundles. In *Advances in Acoustics*, *Noise and Vibration – 2021' Proceedings of the 27th International Congress on Sound and Vibration*, *ICSV 2021* (Vol. 1, pp. 2730–3736). International Institute of Acoustics & Vibration.

Swinburn, T. K., Hammer, M. S., & Neitzel, R. L. (2015). Valuing quiet: An economic assessment of U.S. environmental noise as a cardiovascular health hazard. *American Journal of Preventive Medicine*, *49*(3), 345–353. https://doi.org/10.1016/j.amepre.2015.02.016

Tang, Y. C., & Cheng, H. D. (2025). Analysis and verification of optimization of micro-perforated panels' sound absorption using the Taguchi method. *Journal of the Acoustical Society of America*, *157*(4), 3099–3111. https://doi.org/10.1121/10.0036504

Xie, H., & Lyu, Y. (2014). Sound absorption characteristics of the perforated panel resonator with tube bundles. In *21st International Congress on Sound and Vibration 2014*, *ICSV 2014* (Vol. 1, pp. 5010–5015). International Institute of Acoustics and Vibrations.

Zhao, Y., Guo, Z., Ye, J., Li, Z., Zeng, K., Lu, X., & Wang, Z. (2025). Mechanism of effective depth enhancement and broadband sound absorption optimization in nested resonators with multiple cross-sections. *Materials and Design*, *255*, Article 114140. https://doi.org/10.1016/j.matdes.2025.114140